MEMS–Based Uncooled Infrared Bolometer Arrays–A Review

3 authors, including:

Christian Vieider
Ascatron AB

28 PUBLICATIONS   **386** CITATIONS

SEE PROFILE

Henrik Jakobsen
University College Southeast Norway

77 PUBLICATIONS   **908** CITATIONS

SEE PROFILE

Some of the authors of this publication are also working on these related projects:

Project   photoenegy conversion Of TiO2 nanotubes View project

Project   Create new project "Acreo, Bolometer" View project

MEMS-Based Uncooled Infrared Bolometer Arrays – A Review

Frank Niklaus

KTH - Royal Institute of Technology, Microsystem Technology Lab, 10044 Stockholm, Sweden and
Faun AB, SE-18361, Sweden
Tel: +46 8 76 216 73 49, Fax: +46 8 10 08 58, frank.niklaus@ee.kth.se

Christian Vieider

Acreo AB, Electrum 236, 164 40 Kista, Sweden
Tel: +46 8 632 78 45, Fax: +46 8 750 54 30, christian.vieider@acreo.se

Henrik Jakobsen

Vestfold University College, Institute for Microsystem Technology, 3103 Tønsberg, Norway
Tel: +47 330 37 711, Fax: +47 330 31 03, henrik.jakobsen@hive.no

Abstract

Uncooled infrared bolometer arrays have become the technology of choice for low-cost infrared imaging systems used in applications such as thermography, firefighting, driver night vision, security and surveillance. Uncooled infrared bolometer arrays are reaching performance levels which previously only were possible with cooled infrared photon detectors. With a continuously increasing market volume (> 100 000 units per year to date), the cost for uncooled infrared imaging chips are decreasing accordingly. In this paper we give an overview of the historical development of uncooled infrared bolometer technology and present the most important bolometer performance parameters. The different technology concepts, bolometer design approaches and bolometer materials (including vanadium oxide, amorphous silicon, silicon diodes, silicon-germanium and metals) are discussed in detail. This is followed by an analysis of the current state-of-the-art infrared bolometer technologies, the status of the infrared industry and the latest technology trends.

Keywords: uncooled infrared bolometer arrays, microbolometer, MEMS, infrared detector, focal plane array, IR, FPA

1. Introduction

The word bolometer originates from the Greek word bolē and means ray-meter [1]. Bolometers are thermal infrared sensors that absorb electromagnetic radiation and thus increase their temperature. The resulting temperature increase is a function of the radiant energy striking the bolometer and is measured with e.g. the thermoelectric, pyroelectric, resistive or other temperature sensing principles. In the context of uncooled infrared imaging technologies, the term "infrared bolometer" usually refers to resistive microbolometers in which the temperature increase is measured by a resistance change. This review paper focuses on resistive microbolometers and does not include other thermal infrared detectors such as e.g. thermocouples [2], pyroelectric [3] and ferroelectric [4] uncooled infrared detectors. In the first bolometer, invented by the American scientist Samuel P. Langley in 1880 [5], a Wheatstone bridge was used along with a galvanometer that produced a deflection proportional to the intensity of radiation for small deflections. A later bolometer [6] consists of four platinum gratings, each of which is made of a series of strips, inserted in the arms of a resistance bridge. A number of other resistive thin film bolometers have been proposed from 1947 to 1980 [7-11]. The first thin film resistive micobolometers were proposed by R. Hartmann [12] and K.C. Liddiard [13, 14] in 1982 and 1984 respectively. Uncooled infrared microbolometers and focal plane array technology developed at Honeywell has been published since the late 80's [15-22]. A number of books, book chapters and review articles on infrared technology, including uncooled infrared bolometers, have been published in recent years [23-29]. Uncooled infrared bolometers have become the dominating technology for the majority of commercial and military infrared imaging applications. Some of the most common infrared imaging applications are thermography, night vision (military, commercial and automotive),

mine detection, reconnaissance, surveillance, fire fighting, medical imaging, predictive maintenance and industrial process control.

2. Infrared Bolometer Operation and Figures of Merit

Infrared radiation is part of the electromagnetic spectrum with wavelengths above the visible spectrum, ranging from 0.75 μm to 1000 μm. The infrared spectrum where the infrared transmission is allowed by the atmosphere is in the 3-5 μm wavelength region (mid wave infrared, MWIR) and in the 8-14 μm wavelength region (long wave infrared, LWIR) as can be seen in Figure 1a. The emitted radiation of a black body with a temperature of 300 K has an intensity peak at a wavelength of about 10 μm as can be seen in Figure 1b. The radiation flux from real objects varies, depending on the emissivity of the surface of the object.
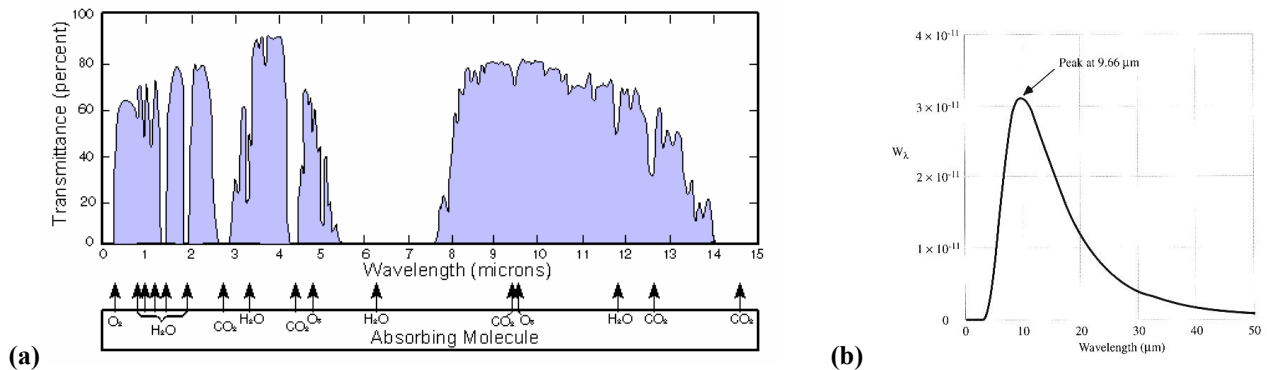

(a) **(b)**

Figure 1: (a) *Plot of atmospheric transmittance in part of the infrared region [30] and (b) radiant flux versus infrared wavelength for a black body with a temperature of 300 K [31].*

Ensembles of infrared detectors in two-dimensional arrays are called focal plane arrays (FPAs). Figure 2a shows a typical infrared bolometer pixel and a two-dimensional bolometer focal plane array. Figure 2b shows a schematic of a typical assembly of an infrared imaging system with a FPA and an infrared lens system. For the majority of infrared imaging applications the bolometers are optimized to detect radiation in the 8-14 μm wavelength region. There are also bolometers that are optimized for broad-band detection in both the 3-5 μm and the 8-14 μm wavelength region at the same time [33]. Bolometers absorb the incident radiation and cause the thermally isolated bolometer membrane to increase its temperature. The temperature change correlates to the energy of the absorbed radiation and is measured by a change of the electrical resistance of the bolometer thermistor material. For microbolometers, a temperature increase of 1 K in the object typically results in a temperature increase in the bolometer membrane on the order of 4 mK [25].
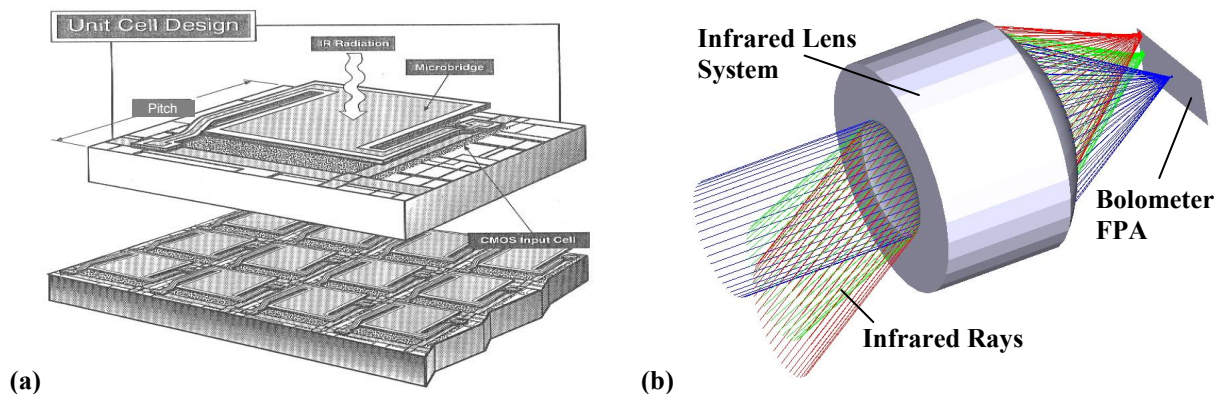

(a) **(b)**

Figure 2: (a) *Schematic drawing of a monolithically integrated infrared bolometer focal plane array (FPA) [32] and (b) placement of a focal plane array with an infrared lens system.*

Important figures of merit for uncooled infrared bolometer and system performances are the noise equivalent temperature difference (NETD), the responsivity ($\Re$), the noise equivalent power (NEP) and the detecitivity (D*) [24, 25, 34-40]. The noise equivalent temperature difference (NETD) is one of the most important performance parameters for infrared imaging systems and is defined as the difference in temperature between two side-by-side blackbodies of large lateral extent which, when viewed by the infrared imaging system, gives rise to a difference in signal-to-noise-ratio of 1 in the electrical outputs of the two halves of the array, viewing the two blackbodies. The responsivity ($\Re$) is defined as the output signal voltage or output signal current of an infrared bolometer pixel per incident radiant power on the pixel. The noise equivalent power (NEP) is the incident infrared power on an infrared bolometer pixel that generates a signal output that is equal to the root-mean-square (RMS) noise output (i.e. resulting in a signal to noise ratio of 1). The detecitivity (D*) is defined as the root-mean-square signal-to-noise ratio of a 1 Hz bandwidth per unit root-mean-square incident radiant power per square root of bolometer area. The detectivity provides information that is equivalent to the noise equivalent power (NEP), but with the possibility to compare bolometer pixels of the same type but with different pixel areas.

Infrared imaging systems based on uncooled bolometer arrays can reach NETDs of below 25 mK with a F-number of the infrared optics of F = 1 [29, 32, 37, 41, 42]. For conventional infrared imaging systems based on uncooled bolometer arrays with column based read-out designs and integrated analogue-to-digital conversion (ADC), the NETD including the contributing NETD parts can be expressed by [38, 39]

$$NETD^2 = NETD_{\frac{1}{f}}{}^2 + NETD_{Johnson}{}^2 + NETD_{thermal}{}^2 + NETD_{ROIC}{}^2 \qquad (Eq.1)$$

where the total NETD consists of the $NETD_{1/f}$ from the 1/f-noise of the bolometers, the $NETD_{Johnson}$ from the Johnson noise of the bolometers, the $NETD_{thermal}$ from the thermal fluctuation noise of the bolometers including temperature fluctuation noise from radiation heat exchange, and the $NETD_{ROIC}$ from the read-out integrated circuit (ROIC) related noise. For the assumption that the bolometer temperature and the surrounding (background) temperature are equal, the contributing NETD parts can be estimated by equations 2 to 6

$$NETD_{\frac{1}{f}} = \left(4 \cdot \frac{F^2}{\phi_{\lambda1-\lambda2} \cdot \left(\frac{\Delta P}{\Delta T}\right)_{\lambda1-\lambda2}} \right) \cdot \frac{G}{\beta \cdot A \cdot \varepsilon_{\lambda1-\lambda2}} \cdot \frac{\sqrt{\frac{K}{\upsilon}} \cdot \sqrt{\ln\left(\frac{x_l \cdot f_i}{f_s}\right)} \cdot \sqrt{1 + \omega^2 \cdot \left(\frac{C}{G}\right)^2}}{TCR} \qquad (Eq.2)$$

$$NETD_{Johnson} = \left(4 \cdot \frac{F^2}{\phi_{\lambda1-\lambda2} \cdot \left(\frac{\Delta P}{\Delta T}\right)_{\lambda1-\lambda2}} \right) \cdot 2 \cdot \sqrt{k} \cdot \frac{G}{\beta \cdot A \cdot \varepsilon_{\lambda1-\lambda2}} \cdot \frac{\sqrt{T_1} \cdot \sqrt{R_{bol}} \cdot \sqrt{x_l \cdot f_i} \cdot \sqrt{1 + \omega^2 \cdot \left(\frac{C}{G}\right)^2}}{TCR \cdot U_{bias}} \qquad (Eq.3)$$

$$NETD_{thermal} = \left(4 \cdot \frac{F^2}{\phi_{\lambda1-\lambda2} \cdot \left(\frac{\Delta P}{\Delta T}\right)_{\lambda1-\lambda2}} \right) \cdot \sqrt{k} \cdot \frac{G}{\beta \cdot A \cdot \varepsilon_{\lambda1-\lambda2}} \cdot \frac{T_1}{\sqrt{C}} \qquad (Eq.4)$$

$$NETD_{ROIC} = \left(4 \cdot \frac{F^2}{\phi_{\lambda1-\lambda2} \cdot \left(\frac{\Delta P}{\Delta T}\right)_{\lambda1-\lambda2}} \right) \cdot \frac{G}{\beta \cdot A \cdot \varepsilon_{\lambda1-\lambda2}} \cdot \frac{(R_{ROIC} + R_{bol}) \cdot \sqrt{1 + \omega^2 \cdot \left(\frac{C}{G}\right)^2}}{TCR \cdot U_{bias} \cdot R_{ROIC}} \cdot V_{ROIC} \qquad (Eq.5)$$

$$V_{ROIC} = \sqrt{V_{amp}(x_l \cdot f_i)^2 + \frac{V_Q^2}{12} + \left(\frac{R_{ROIC} \cdot R_{bol}}{R_{ROIC} + R_{bol}}\right)^2 \cdot I_{ROIC}(x_l \cdot f_i)^2} \qquad (Eq.6)$$

where F is the F-number of the infrared optics, $\phi_{\lambda1-\lambda2}$ is the transmission of the infrared optics in the wavelength interval from λ1 to λ2, G is the thermal conduction between each bolometer and its surroundings, C is the heat capacity of the

bolometer pixel, TCR is the temperature coefficient of resistance of the resistive bolometer material (dependent on the bolometer temperature), K is the 1/f noise constant of the resistive bolometer material, υ is the volume of the resistive bolometer material, T_1 is the bolometer membrane temperature, R_{bol} is the bolometer resistance at the temperature T_1, β is the bolometer pixel fill factor, A is the bolometer pixel area (pixel pitch), $\varepsilon_{\lambda1-\lambda2}$ is the infrared absorption rate of the bolometer membrane in the wavelength interval from $\lambda1$ to $\lambda2$, x_l is the amount of bolometer pixels per column (number of bolometers that are read-out during one imaging frame), f_i is the image read-out frequency (imaging frame rate), f_s is the shutter or uniformity correction frequency for the bolometer array, U_{bias} is the bolometer bias voltage, R_{ROIC} is the input impedance (resistance) of the ROIC, V_{ROIC} is the total noise voltage of the ROIC, V_{amp} is the input reference noise voltage of the ROIC (depending on the ROIC architecture, typically a function of $x_l \cdot f_i$), V_Q is the input reference analogue-to-digital quantization interval, I_{ROIC} is the current noise from the ROIC input including the bolometer bias current source (depending on the ROIC architecture, typically a function of $x_l \cdot f_i$), $\left(\dfrac{\Delta P}{\Delta T}\right)_{\lambda1-\lambda2}$ is the temperature contrast in the wavelength interval from $\lambda1$ to $\lambda2$, ω is the modulation frequency of the infrared signal from the image scene, and k is the Boltzmann constant. The above NETD equations are valid for the assumption that the bolometer read-out integration frequency f_r is much larger than the thermal bolometer integration frequency f_{bol} with

$$f_r = x_l \cdot f_i \qquad\qquad\qquad (Eq.7)$$

$$f_{bol} = \frac{1}{4 \cdot \tau} \qquad\qquad\qquad (Eq.8)$$

$$\tau = \frac{C}{G} \qquad\qquad\qquad (Eq.9)$$

where τ is the thermal time constant of a bolometer pixel, f_r is the bolometer read-out integration frequency and f_{bol} is the thermal bolometer integration frequency.

3. Bolometer Design and Manufacturing

3.1 Geometrical and optical bolometer design

To design uncooled infrared bolometer arrays with a high sensitivity (low NETD), a number of design features and trade-offs have to be considered as can be seen from equations 1 to 9. Some of the most important bolometer design parameters are a low thermal conductance between the bolometer and its surrounding, a high absorption of the infrared radiation including a large absorbing area, a bolometer temperature sensing material with a high temperature coefficient of resistance (TCR) and low 1/f noise properties and a sufficiently low bolometer thermal time constant. At the same time it is important for commercial infrared imaging applications, that the bolometer pixels are as small as possible with reported pixel pitches being as small as 17 µm x 17 µm [33, 43, 44]. Small bolometer pixels allow the implementation of high-resolution focal plane arrays at acceptable cost. The cost for both the FPA chip and for the infrared optics is reduces by reducing the active area of the FPA.

Figure 3a shows details of a typical bolometer design. To obtain a small thermal conduction between the bolometer and its surroundings, the bolometer legs are long, have a small cross-sectional area and consist of materials with a low thermal conductivity. The legs typically contain a thin metal layer to provide electrical contact between the bolometer material and the read-out electronics. Thermal conduction through the bolometer legs can be as low as $3.5 \cdot 10^{-8} \dfrac{W}{K}$ [32].

In addition, conventional bolometers are operated in a vacuum package to minimize the thermal conduction between the bolometers and their surroundings through the surrounding gas. The vacuum atmosphere in which the bolometers are operated is typically on the order of 0.01 mbar [45].

The bolometer pixel fill factor defines the portion of the bolometer pixel area that is used to absorb the incident infrared radiation. The remaining area of the bolometer pixel is consumed by the bolometer legs, the space between the bolometer and the neighboring bolometer membranes, and the vias that connect the bolometer and the read-out integrated circuit wafer as can be seen in Figure 3a. Conventional single-level infrared bolometer arrays typically have a fill factor between 60 % and 70 % [32, 37]. To increase the bolometer pixel fill factor, two-layer bolometer designs (umbrella

designs) as shown in Figure 3b have been reported that reach fill factors of up to 90 % [46, 47]. The bolometer legs, and in some cases the temperature sensing material [33] are placed underneath the absorbing bolometer membrane. Such umbrella designs have been implemented in bolometer FPAs with very small pixel sizes [33, 46].
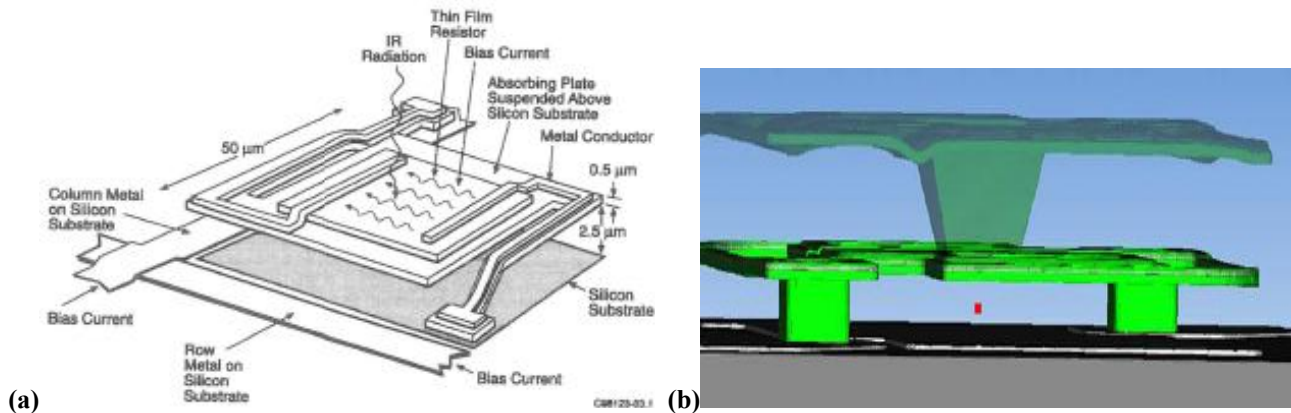

(a) (b)

Figure 3: *(a) Details of a typical single-level bolometer design [24] and (b) example of a two-level (umbrella) design for improved pixel fill factor [33].*

To provide a high absorption of the radiation in the bolometer membrane, conventional bolometers contain resonant optical cavity (Fabry-Perot) structures that are optimized for the targeted wavelength interval as depicted in Figure 4. The most commonly used resonant optical cavity design is shown in Figure 4a, in which the infrared mirror (typically aluminium) of the resonant optical cavity is placed on the surface of the underlying substrate (the ROIC) and the bolometer membrane is placed at a distance of $\frac{\lambda}{4}$ from the mirror surface on the substrate. Thus, a high fraction of the incident infrared radiation at a specific wavelength λ is absorbed in the bolometer membrane [37]. For a targeted wavelength interval of 8 μm to 14 μm, the distance between the bolometer membrane and the mirror on the substrate is typically about 2 μm to 2.5 μm [37, 42]. A second type of resonant optical cavity design is shown in Figure 4b, in which the resonant optical cavity is part of the bolometer membrane. The mirror of this type of resonant optical cavity is placed at the lower surface of the bolometer membrane and the thickness of the bolometer membrane defines the resonant optical cavity. The membrane thickness is typically set to $\frac{\lambda_x}{4}$, where λ_x is the wavelength of the targeted infrared radiation in the bolometer membrane material(s) [48]. Most commercial bolometer FPAs make use of the optical cavity design shown in Figure 4a since it allows thinner bolometer membranes with a lower heat capacity, which in turn can be used to minimize the thermal bolometer conductance and the resulting NETD. The top metal layer (e.g. titanium nitride) of the Fabry-Perot cavity usually has a target sheet resistance of 377 Ω/sq to reach optimum performance of the Fabry-Perot cavity in the wavelength interval of 8 μm to 14 μm [48].
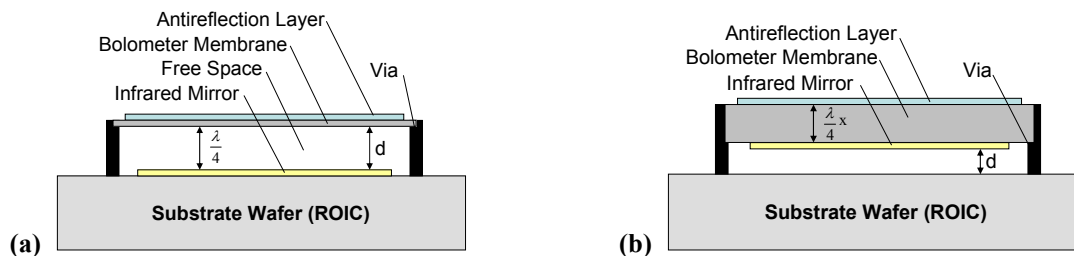

Figure 4: *Cross-sectional image of two bolometer designs with resonant optical cavities for high absorption of the incident radiation.*

3.2 Bolometer focal plane array manufacturing techniques

The most commonly used manufacturing approach for uncooled infrared bolometer FPAs is monolithic integration [37, 41, 42, 45, 49] as shown in Figure 5. In monolithic integration, the ROIC is pre-manufactured and the bolometer

materials are subsequently deposited and patterned on the ROIC wafer. Typically, a high-temperature stable polyimide is used as the sacrificial layer. In the final step, the polyimide layer is sacrificially removed in an oxygen plasma to obtain the free-standing, thermally isolated bolometer membranes. All commercially available vanadium oxide and amorphous silicon bolometer FPAs are monolithically integrated on top of the ROICs. Monolithic integration is a cost-efficient and well-established post CMOS process in which the electronics for the signal read-out can be efficiently placed underneath and beside the bolometer membranes. One potential disadvantage of monolithic integration is that the deposition process for the temperature sensing bolometer material is limited to about 450ºC and does not allow the deposition of mono-crystalline materials. Process temperatures higher than 450ºC risk damaging the ROIC. This can make the optimization of the temperature sensing bolometer material difficult.
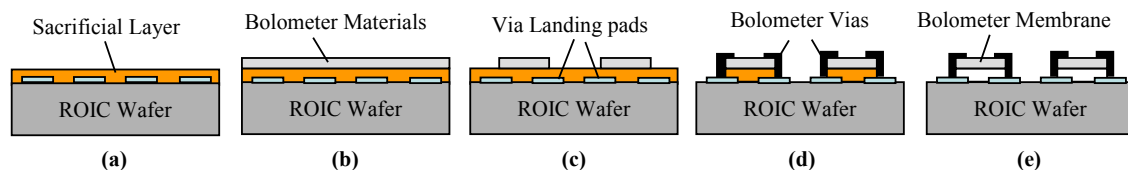

Figure 5: *Monolithic integration for uncooled infrared bolometer arrays: (a) deposition of sacrificial layer on ROIC wafer; (b) deposition of bolometer materials; (c) patterning of bolometer materials; (d) via formation; (f) etching of sacrificial layer.*

Bulk micromachining is a second alternative to manufacture uncooled infrared bolometers [50] as shown in Figure 6. In bulk micromachining, the bolometers are formed in the substrate surface of a wafer. Subsequently, the substrate is selectively etched underneath the bolometers to thermally separate them from the rest of the substrate. The bulk micromaching processes can be implement before, in between or after processing the wafers e.g. in a CMOS line to implement the necessary electronic components. Commercial infrared bolometer arrays that are manufactures using bulk micromachining techniques are diode bolometers. The advantage of bulk micromachining is that the electronics and the bolometers can typically be manufactured in a standard CMOS line. The free-etching of the bolometers can then be done in a single post CMOS process step. A disadvantage of bulk-micromachining is that the electronics for the signal read-out can not be placed underneath the bolometer membranes, but has to be placed beside the bolometers. This usually reduces the bolometer fill factor.
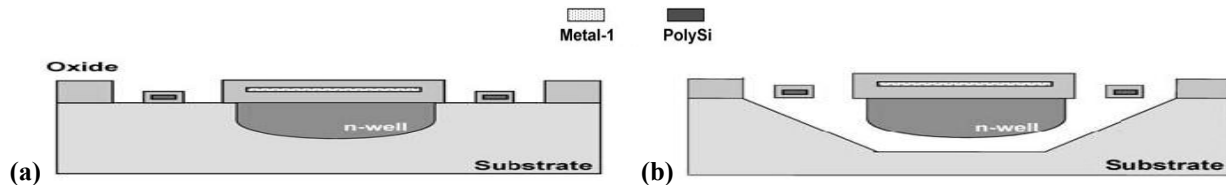

Figure 6: *Bulk micromachining for uncooled infrared bolometer arrays: (a) Formation of the bolometer and the electronics for signal read-out (typically side-by-side); (b) selective etching of the bulk material underneath the bolometer membrane [50].*
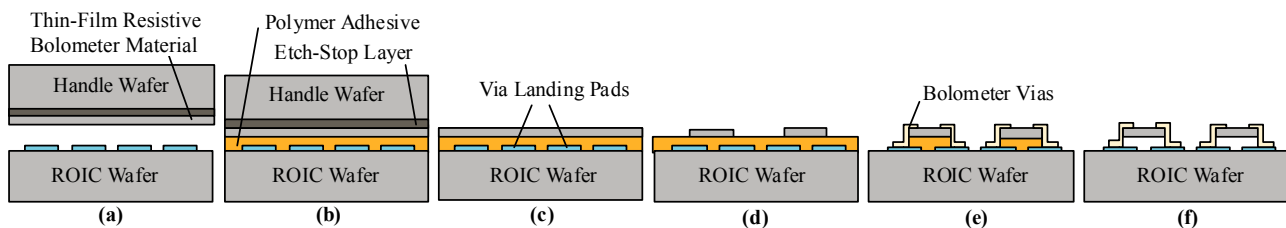
Figure 7: *Heterogeneous 3D integration for uncooled infrared bolometer arrays: (a) separate fabrication of ROIC wafer and handle wafer with resistive bolometer material; (b) adhesive wafer bonding; (c) thinning of handle wafer; (d) bolometer definition; (e) via formation; (f) sacrificial etching of polymer adhesive.*

Heterogeneous three dimensional (3D) bolometer integration has been proposed for the integration of high-performance mono-crystalline temperature sensing bolometer materials on ROICs [48, 51-56]. In 3D bolometer integration, the bolometer materials are deposited on a separate handle wafer. The materials are then transferred from the handle wafer to

the ROIC wafer using low-temperature adhesive wafer bonding in combination with sacrificial removing of the handle wafer as shown in Figure 7c. The achievable bolometer dimensions are identical to the ones made with conventional monolithic micromachining techniques. The advantage of 3D bolometer integration is that it allows the use of high-performance mono-crystalline temperature sensing bolometer materials on top of standard ROICs. A 3D bolometer integration process is currently being implemented in a project with consortium partners Autoliv, Infineon Technologies SensoNor, Umicore, VITO, KTH-MST and Acreo [53-55].

3.3 Bolometer temperature sensing materials

The selected bolometer temperature sensing material has a large influence on the sensitivity (NETD) of the bolometer. A high temperature coefficient of resistance (TCR) and a small 1/f noise constant are desirable material properties as can be seen from equations 1 to 9. At the same time, it must be possible to integrate the temperature sensing material together with signal read-out electronics (e.g. a CMOS wafer) in a cost efficient way. Today, the most common bolometer temperature sensing materials are vanadium oxide (VO_x), amorphous silicon (α-Si) and silicon diodes. The NETD of state-of-the-art uncooled infrared bolometer FPAs is typically limited by the 1/f noise from the bolometer temperature sensing material [32, 36]. The 1/f noise constant is a material parameter that can vary several orders of magnitude for different materials and even small variations of the material composition can dramatically change the 1/f noise constant [35]. For most materials 1/f noise constant is not very well documented in literature, however, mono-crystalline materials can have a significantly lower 1/f noise constant as compared to amorphous or poly-crystalline materials. Thus, one way to reduce the NETD of a bolometer FPA may be the use of mono-crystalline temperature sensing bolometer materials with a low 1/f noise constant [32, 36, 38, 39].

3.3.1 Vanadium oxide (VOx)

The vanadium oxide thin films that are used have TCR in the range 2 %/K and 3 %/K at room temperature [57, 58] and is today used in a variety of bolometer products. There are many phases in vanadium oxides, such as VO_2, V_2O_5 and V_2O_3. They undergo transition from an insulator or semiconductor to a metal phase at a specific temperature. Single-crystal VO_2 and V_2O_5 have TCR above 4 %/K, but are difficult to make. Commonly used thin film depositions techniques such as evaporation and sputtering will give amorphous or polycrystalline films. V_2O_5 can be formed by ion beam from vanadium metal target in high O_2 partial pressure, but its resistance at room temperature is very high. V_2O_3 has low formation energy and undergoes a transition from semiconductor to metal phase at low temperature, so its resistance is very low at room temperature. Because high electrical resistance of a device results in a high level of noise, the use of the V_2O_3 phase showing low resistance is important to the fabrication of low-noise microbolometers.

Vanadium oxide films can be prepared by a variety of methods, including the annealing and oxidation of evaporated vanadium under controlled conditions, reactive RF sputtering [49, 60] and pulsed laser deposition [61]. Y-H. Han et. al. [62] have shown that through the formation of a sandwich structure of V_2O_5, V and V_2O_5 by a conventional sputter method, a controlled mixed phase of VO_x with good electrical properties by can be formed by post-annealing in oxygen. Several groups are active to find processes to obtain high TCR in combination with sufficient low sheet resistance for good noise performance. Y. Lv et. al. [63] have obtained TCR value about 4.4 %/K and low sheet resistance <20 kΩ/square by using facing target sputtering and heat treatment. The performance limits of uncooled VO_x microbolometer focal plane arrays are reported in [32]. It is reported [64-66] that bolometer characteristics can be improved by using vanadium-tungsten oxide made by low temperature oxidation of vanadium-tungsten metal films. M. Soltani et. al. [67] report a strong effect of Ti–W co-doping on both the optical and electrical properties of vanadium dioxide thin films grown by a reactive pulsed laser deposition. They achieved films with TCR 5.12 %/K.

3.3.2 Amorphous silicon (α-Si)

Amorphous silicon (α-Si) is extensively described and used in a large variety of products such as active layer in thin-film transistors for liquid crystal displays, small area solar powered photovoltaic devices for consumer products and large area power solar cells. A description of amorphous silicon microbolometers technology was published by A. J. Syllaios et. al. in 2000 [68]. The hydrogenated amorphous silicon (α-Si) microbolometer arrays that have been developed take advantage of the high TCR, relatively high optical absorption coefficient and the advantage that they can be manufactured using silicon fabrication compatible processes. TCR up to about 3 %/K at room temperature have been reported [69]. Bolometers made of α-Si can consist of very thin memebranes, which allows for a low thermal mass and consequently, for bolometers with a low thermal conductance while maintaining a fixed bolometer time constant.

Hydrogenated amorphous silicon (α-Si) is a thin–film amorphous material that can only be produced by a non-equilibrium process, such as plasma-enhanced chemical vapor deposition (PECVD) or sputtering. The properties are therefore a direct consequence of the deposition process. The TCR and sheet resistance depends on material properties such as doping concentration, deposition temperature and annealing. α-Si can be deposited at very low temperatures, as low as 75 °C, which allows for deposition on not only silicon and glass, but plastic as well, making it a candidate for a roll-to-roll processing technique. The relatively lower electronic performance of low-temperature α-Si devices could be compensated by the cheaper production, for future, ultra-low-cost, high-volume applications.

3.3.3 Silicon diodes
The temperature coefficient of the forward voltage of a pn-junction or Schottky barrier junction can be used as sensing principle for the temperature caused by absorption of IR radiation. With a forward voltage of about 0,7 V for silicon pn-diodes and about 0,6 V for silicon Schottky-diodes and a voltage change with temperature in the range 1-2 mV/K give a temperature coefficient of about 0.2 %/K, an order of magnitude lower than the best resistive devices. An advantage of using diodes may be the possibility this gives for smaller pixel size because diodes can normally be made on smaller areas than resistors. The bolometer diodes can potentially be manufactured in standard CMOS lines. The use of amorphous silicon thin film transistors (α-Si TFT) as the active elements has been reported by L. Dong et. al. [70, 71]. The TFT used had a high temperature coefficient of its drain current in the range 1.5 to 6.5 %/K at room temperature.

3.3.4 Other Bolometer Materials
A simple alternative for temperature sensing material are thin film metals. They are easy to integrate with CMOS ROIC process and the 1/f noise is low. TCR is unfortunately also very low (e.g. Titanium up to 0.35 %/K [72]), which results in low performance detectors [73]. Titanium is preferred due to its low thermal conductance.
An alternative to α-Si are different types of amorphous germanium-silicon-oxygen compounds ($Ge_xSi_{1-x}O_y$) grown by reactive sputtering in an Ar or Ar:O_2 environment [74, 75, 76], or by plasma enhanced chemical vapor deposition [77]. The Ge content is in the order of 85%. TCR values up to 5.1 %/K have been reported, but the relatively high 1/f noise lower the potential detector performance. The advantage is lower thermal conductance.
Another alternative is poly crystalline silicon germanium (SiGe) with approximately 30% Ge. Very thin membranes (100nm) can be produced using standard CMOS processes, e.g. reduced-pressure chemical vapor deposition (CVD). Due to the high deposition and annealing temperatures has the membrane however to be manufactured before metallization [78]. Other reported alternatives for poly-SiGe film are molecular-beam deposition [79], or ultra-high vacuum vapor deposition [80]. The detector performance that can be obtained is up to now lower than e.g. VO$_x$ due to the higher 1/f noise of the poly crystalline material. By growing very thin (nm) Si/SiGe multi-layers epitaxially is it possible to create a single crystalline material with integrated valence barriers. The TCR can thereby be high (3.3 %/K) and simultaneously, the high quality crystalline material provides very low 1/f-noise characteristics. Advantageous is also the stability of the quantum well thermistor material, which e.g. allows standard metallization annealing temperatures [54, 81].
Wide-band gap materials have also been investigated, e.g. PECVD deposited amorphous silicon carbide [82] and photo-chemical vapor deposition of nanocrystalline silicon carbide [83]. TCR can be controlled with the deposition parameters and e.g. be varied between 0.7 and 2.3 %/K. The noise level increase however with higher TCR and a trade-off has to be made to achieve maximum performance.
Another type of thermistor materials are semiconducting YBaCuO. The material can also be designed with pyroelectric properties depending on the oxygen stoichiometry. Deposition can be made at low temperature with magnetron sputtering, and TCR values between 2.8 and 4 %/K have been reported [84, 85]. Perovskite metal-oxide manganites with colossal magneto resistance effect (CMR) have also been proposed for thermal imaging. Very high TCR values can be obtained around the phase transition temperature when changing from semiconductor to metal. At room temperature has a TCR of 4.4 %/K been obtained [86].
A recently reported material with performance claimed to be compatible with VO$_x$ is thin-film carbon. It is made by depositing a parylene layer and pyrolyze it to carbon at 800°C [87].

3.4 Bolometer vacuum package
Bolometers need to be packaged in vacuum for best performance. Therefore, conventional bolometers operate with vacuum levels < 0.01 mbar [47]. Important requirements for the packaging of bolometer arrays are: good and reliable hermetic seal; integration of IR window material with good infrared transmission; and high yield low cost packaging. Both reliability and cost of MEMS is heavily related to the encapsulation techniques chosen. For MEMS based

bolometers, packaging may be done at chip level or wafer level. The most common way of packaging is to build the bolometer chip into a hermetic metal or ceramic package with an IR-transmitting lid build into the package cap.

The need for packaging of microbolometers in vacuum is related to the fact that heat loss due to thermal conduction from the bolometer structure through the gas gap to the substrate underneath will increase the NETD as indicated in equations 1-9. At higher pressure levels the thermal conductance G_{air} through the air-gap can be estimated to be:

$$G_{air} = k_{air}\, A/d \qquad\qquad (Eq.\ 10)$$

where k_{air} is the thermal conduction for the air, A is the area of the bolometer plate and d is the distance between the plate and the substrate. X. He et al. [88] have measured the typical thermal conductance and heat capacitance of a microbolometer as a function of pressure at room temperature on test structures. Their results shows that thermal conduction through the gas starts to have an effect from a pressure in the range 0.1 mbar for a device with pixel area 50 μm x 50 μm and an air-gap of 20 μm.

An important advantage for MEMS based bolometer arrays is the possibility this technology offers for low cost wafer level vacuum packaging with methods that has become available the last few years. Several alternative methods for wafer level packaging are already developed by the MEMS industry. Hermetic methods include low temperature fusion bonding, anodic bonding, glass frit bonding, and metal based bonding that includes thermo-compression bonding, eutectic bonding and soldering. Good descriptions of these methods will be available in a new handbook for MEMS [89].
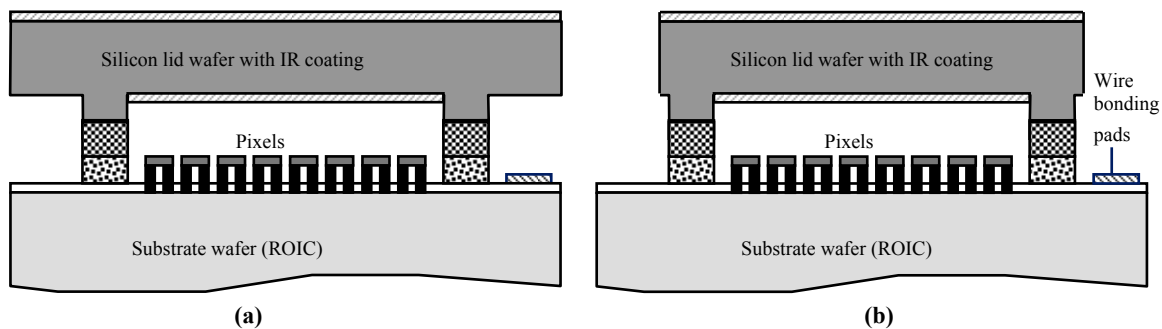

Figure 8: *Principle cross-sectional of wafer level packaging of silicon lid wafer with window areas onto ROIC wafer with bolometer pixels (a) after wafer level sealing and (b) after release of wire bonding areas by sawing.*

For a specific new volume automotive application, we develop a wafer scale package to form lids with silicon IR-window over the bolometer pixel [55]. This technology allows the pixels to be packaged in a hermetic cavity with the electrical contacts outside the cavity at low cost. As a result, this allows the bolometer chip to be integrated directly to the camera housing, hereby reducing the system cost substantially. The inherently good detector performance developed allows us to use a lower vacuum without compromising overall performance too much. This enables good long term stability and makes the use of getter materials and custom processes obsolete. Figure 8 shows the principles of the wafer scale packaging technology that is being developed. The cap-wafer material (window) is made in single-crystal silicon wafers with low oxygen concentration to obtain good IR transmission over the whole wavelength range 8-14 μm. The window areas are made by deep reactive-ion etching. Standard antireflection coating is deposited on both sides of the window areas to obtain windows without any significant degradation of the final effective NETD. A seal ring is added on the frame areas of the ROIC wafer. The cap-wafer is then aligned and attached to the ROIC wafer with the pixels and sealing take place in vacuum. After sealing, the areas on the cap-wafer around the pixel areas are removed by standard wafer dicing saw in order to release the wire bonding pads. The process sequence for the wafer scale packaging allows building of additional thin-film getter structures and Pirani gauge vacuum sensors into each device. Hereby vacuum pressure < 0.01 mbar can be obtained and open up for applications requiring better NETD. Development of specific methods to measure the quality of the vacuum both on wafer level and in the final devices are investigated. Establishing manufacturing schemes by using accelerated testing for checking the actual gas pressure and bonding consistency will hereby be made possible at low cost. Wafer-level vacuum packaging may be an important factor in bringing commercialization of micro-bolometer arrays into low-cost, high volume applications such as home, industry, automotive and environmental monitoring.

4. Bolometer Read-Out Integrated Circuits (ROICs)

Bolometer read-out integrated circuits allow measuring the very small resistance changes of individual bolometers that are part of large bolometer arrays. As can be seen from equations 1 to 9, the noise voltage from the ROIC should be sufficiently low to not be the domination noise contribution to the NETD. To measure the resistance change of a bolometer, the ROIC applies a bias voltage which causes a temperature increase (offset) in the bolometer membrane. As a result of the bolometer self-heating, the ROIC is required to handle a higher dynamic range. Column parallel read-out architectures with integrated AD conversion are commonly used in commercial FPAs [32, 90-92]. Early FPAs used thermo-electric-coolers (TEC) to stabilize the FPA chip at a fixed temperature and to provide a low noise voltage. However, modern FPAs have implemented design features that tolerate and compensate for a floating chip temperature in the specified temperature range [92]. Thus, today many infrared cameras do not require a TEC for temperature stabilization for the FPA chip.

5. Commercial and State-of-the-Art Infrared Bolometer Arrays

Today, the dominating suppliers of high-performance uncooled infrared bolometer arrays are Flir Systems in USA, L-3 in USA, Ulis in France, BAE Systems in USA and DRS in USA. Other suppliers include Raytheon in USA, Mitsubishi in Japan, NEC in Japan and SCD in Israel. Commercially available bolometer arrays are either made from vanadium oxide (VO_x), amorphous silicon (α-Si) or silicon diodes, with VO_x being the dominating technology. Most commercially available bolometer FPA make use of standard single-level bolometer designs. However, some of the FPAs with very small bolometer pixels that are in the R&D stage, consist of two-layer (umbrella-type) bolometer designs [33, 45]. Figure 9a shows scanning electron microscope (SEM) images of a commercial VO_x bolometer [32] and Figure 9b shows a VO_x umbrella type bolometer [33] that is in the R&D stage. Table 1 shows an overview of the main suppliers, the bolometer technology and specifications for existing products and for bolometer arrays that are in the R&D stage. High-performance uncooled infrared bolometer FPAs are subject to export control under the Wassenaar agreement (www.wassenaar.org/introduction/).

Table 1: Commercial and state-of-the-art R&D uncooled infrared bolometer arrays.

| Company	Bolometer type	Array format (pixels)	Pixel pitch (μm)	Detector NETD (F=1, 20-60 Hz)
FLIR, USA	VO_x bolometer	160x120 - 640x480	25	35 mK
L-3, USA	VO_x bolometer	320x240	37.5	50 mK
	α-Si bolometer	160x120 - 320x240	30	50 mK
BAE, USA	VO_x bolometer	320x240 - 640x480	28	30-50 mK
	VO_x bolometer (standard design)	160x120 - 640x480	R&D: 17	50 mK
DRS, USA	VO_x bolometer (umbrella design)	320x240	25	35 mK
	VO_x bolometer (umbrella design)	320x240	R&D: 17	50 mK
Raytheon, USA	VO_x bolometer	320x240 - 640x480	25	30-40 mK
	VO_x bolometer (umbrella design)	640x512	R&D: 17	50 mK
ULIS, France	α-Si bolometer	160x120, 640x480	25-50	35-100 mK
Mitsubishi, Japan	Si diode bolometer	320x240	25	50 mK
NEC, Japan	VO_x bolometer	320x240	23.5	75 mK
SCD, Israel	VO_x bolometer	384x288	25	50 mK
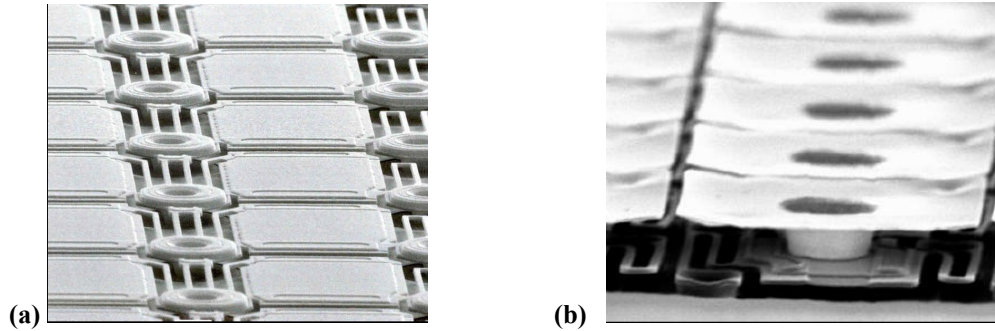
Figure 9: *(a) Commercial VO$_x$ bolometer design with 28 μm x 28 μm pitch from BAE [32] and (b) R&D VO$_x$ bolometer with umbrella design and 17 μm x 17 μm pitch from DRS [33].*

6. Outlook and Future Developments

Development of micro-bolometer technology has the last 5 years continued to dramatically improve performance and resolution. The demonstrated performance is getting closer to the theoretical limit and the gap to photonic detectors is getting smaller. With the advantages regarding weight, power consumption and cost of uncooled technology, micro-bolometer detectors are now produced in larger volumes than all other IR array technologies together.

For the future we can divide the technology requirement and thus development efforts towards the following main market segments:

- High resolution, high performance imaging for surveillance and military – mega pixel arrays with lowest possible NETD.
- Medium resolution, medium performance imaging for automotive and security – 320x240 pixel arrays with a NETD of about 35 mK @F1.
- Low resolution, low performance image based sensing for automotive safety, machine vision and consumables, e.g. 80x30 pixel arrays with a NETD of about 150 mK @F1.

Mass-market application will become the technology driver. State-off-the-art performance is for many applications good enough. This changes the development focus from performance and resolution [33, 43, 44] to low cost production [54, 93, 94]. The main development issues are:

1. Vacuum packaging. First level packaging needs to be integrated in the chip fabrication process using wafer-level technologies and integrated getter materials. This puts additional requirement on high temperature stable detector material.
2. Foundry manufacturing. Only standard materials and fabrication processes that can be used in CMOS and MEMS foundry fabrication. This will open up for many producers and in long term also lower manufacturing cost for smaller series production.
3. Camera module integration. Low resolution arrays will be completely integrated with driving electronics and optics, similar as digital CMOS cameras are produced today.

Initial development cost and complexity of the manufacturing will be of less importance for large volume production, and the production yield and testing requirements will be of larger importance for the final production cost. High-end products for niche markets will in the long run benefit from the achievements and manufacturing infrastructure resulting from the development of mass-market products.

Conclusions

Bolometer arrays have become the technology of choice for low-cost infrared imaging systems used in both civil and military applications. Uncooled infrared bolometer arrays are reaching performance levels which previously only were possible with cooled infrared photon detectors. With a continuously increasing market volume (>100 000 units per year to date), the cost for uncooled infrared imaging chips are decreasing accordingly. The next generation detectors will have a pixel pitch of 17 μm. To increase detector sensitivity, new temperature sensor materials with low 1/f noise and high

TCR are required. The most promising materials are fabricated at relatively high temperature, making post-processing deposition impossible. Heterogeneous 3D integration processes will be developed to solve this issue. Mass-market applications will focus the development on low-cost manufacturing and integration of the whole IR camera module. This requires trade-off optimization of the performance related to cost for each part in the system. As example can the requirement on a very low vacuum pressure be exchanged with a better performing detector material. The manufacturing needs to be aligned with standard CMOS and MEMS foundry processing. This is required for large volume fabrication and the technology development progress will even faster benefit from the achievements continuously gained in the whole semiconductor field.

Acknowledgments

References

[1]   Websters Dictionary.

[2]   A. Schaufelbuhl, N. Schneeberger, U. Munch, M. Waelti, O. Paul, O. Brand, H. Baltes, C. Menolfi, H. Qiuting, E. Doering, M. Loepfe, "Uncooled low-cost thermal imager based on micromachined CMOS integrated sensor array", *Journal of Microelectromechanical Systems*, Vol.10, No.4, pp.503-510, 2001.

[3]   P. Muralt, "Micromachined infrared detectors based on pyroelectric thin films", *Reports on Progress in Physics*, Vol.64, pp.1339-1388, 2001.

[4]   R. Watton, "Ferroelectric IR bolometers - from ceramic hybrid arrays to direct thin film integration", *Ferroelectrics*, Vol.184, pp.141-150, 1996.

[5]   E.S. Barr, "The Infrared Pioneers – III. Samuel Pierpont Langley", *Infrared Physics*, Vol.**3**, pp.195-206, 1963.

[6]   C.B. Aiken, W.H. Carter, F.S. Philips, "The production of film type bolometers with rapid response", *Review of Scientific Instruments*, Vol.17, No.10, pp. 377-385, 1946.

[7]   B.H. Billings, E.E. Barr, W.L. Hyde, "Construction and characteristics of evaporated nickel bolometers", *Review of Scientific Instruments*, Vol.18, No.6, pp.429-435, 1947.

[8]   K. Yosihara, "An investigation of the properties of bolometers made by vacuum evaporation", Science of Light, Vol.5, No.2, pp.29, 1956.

[9]   R.A. Smith, F.E. Jones, R.F. Chasmar, *The Detection and Measurement of Infrared Radiation*, Clarendon Press, Oxford, 1957.

[10]   W. R. Blevin, W.J. Brown, "Large-area bolometers of evaporated gold", *Journal of Scientific Instruments*, Vol.42, No.1, pp.19, 1965.

[11]   J. Gosch, "Thin-film enhances bolometer's sensitivity", *Electronics*, pp.74-76, Feb. 28, 1980.

[12]   R. Hartmann, M. Selders, "High-sensitivity thin-film bolometers", *Proc. Sensor 1982 – Sensor Technology and Temperature Measurement*, pp.102-116, Essen, West Germany.

[13]   K.C. Liddiard, "Thin-film resistance bolometer IR detectors", *Infrared Physics,* Vol.24, pp.57-64, 1984.

[14]   K.C. Liddiard, "Thin-film resistance bolometer IR detectors – II", *Infrared Physics*, Vol.26, pp.43-49, 1986.

[15]   R.A. Wood, J. Carney, R.E. Higashi, T. Ohnstein, J. Holmen, "Advances in uncooled silicon monolithic IR 2D arrays", *Proc. IRIS DSG*, 1988.

[16]   R.A. Wood, R.A. Carlson, R.E. Higashi, N.A. Foss, "Progress in silicon monolithic uncooled IR focal plane arrays", *Proc. IRIS DSG*, 1989.

[17]   R.A. Wood, B.E. Cole, N.A. Foss, C.J. Han, R.E. Higashi, R. Lubke, "Monolithic silicon uncooled focal plane development for high density array development program (HIDAD)", *Proc. IRIS DSG*, 1990.

[18]   R.A. Wood, B.E. Cole, C.J. Han, R.E. Higashi, "Monolithic silicon uncooled focal planes for the HIDAD program", *Proc. IRIS DSG*, 1991.

[19]   R.A. Wood, B.E. Cole, C.J. Han, R.E. Higashi, D. Nielsen, A. Weinstein, "HIDAD – a monolithic silicon uncooled infrared imaging focal plane", *Proc. GOMAC,* 1991.

[20]   R.A. Wood, C.J. Han, P.W. Kruse, "Integrated uncooled infrared detector imaging arrays", Proc. Solid-State Sensor and Actuator Workshop 1992, pp.132-135, Hilton Head Island, USA.

[21] R.A. Wood, N.A. Foss, "Micromachined bolometer arrays achieve low-cost imaging", *Laser Focus World*, pp.101-106, June, 1993.

[22] R.A. Wood, "Monolithic silicon microbolometer arrays", in P.W. Kruse, D.D. Skatrud, *Semiconductors and Semimetals*, Vol.47, pp.45-121, Academic Press, San Diego, USA, 1997.

[23] P.W. Kruse, "Uncooled IR focal plane arrays", *Opto-Electronics Review*, No.7, pp.253-258, 1999.

[24] R.A. Wood, "Uncooled microbolometer infrared sensor arrays", in P. Capper, C.T. Elliott, *Infrared Detectors and Emitters: Materials and Devices*, pp.149-174, Kluwer Academic Publishers, Boston, USA, 2000.

[25] P.W. Kruse, *Uncooled Thermal Imaging. Arrays, Systems, and Applications*, SPIE Press, Bellingham, USA, 2001.

[26] T. Akin, "CMOS-based Thermal Sensors", in H. Baltes, O. Brand, G. K. Fedder, C. Hierold, J. Korvink, O. Tabata, *Advanced Micro and Nanosystems*, Vol.2, pp.280-498, CMOS - MEMS, WILEY-VCH Verlag GmbH & Co. KGaA, Weinheim, CH, 2005.

[27] A. Rogalski, *Infrared Detectors*, Gordon and Breach Science Publishers, Amsterdam, The Netherlands, 2000.

[28] A Rogalski, "Infrared detectors: an overview", *Infrared Physics and Technology*, Vol.43, pp.187-210, 2002.

[29] A. M. Filachev, V. P. Ponomarenko, I. I. Taubkin, M. B. Ushakova, "Infrared focal plane arrays: state of the art and development trends", *Proc. SPIE 2003*, Vol. 5126, pp. 52-85, Moscow, Russia.

[30] Source: U.S. Navy, http://en.wikipedia.org/wiki/Infrared.

[31] G.T.A Kovacs, *Micromachined transducers sourcebook*, McGraw-Hill, Boston, USA, 1998.

[32] M. Kohin, N. Buttler, "Performance limits of uncooled VOx microbolometer focal plane arrays", *Proc. SPIE 2004*, Vol. 5406, pp. 447-453, Orlando, USA.

[33] C. Li, G.D. Skidmore, C. Howard, C.J. Han, L. Wood, D. Peysha, E. Williams, C. Trujillo, J. Emmett, G. Robas, D. Jardine, C.-F. Wan, E. Clarke "Recent development of ultra small pixel uncooled focal plane array at DRS, *Proc. SPIE 2007*, Vol.6542, pp.1Y.1-1Y.12, Orlando, USA.

[34] P.L. Marasco, E.L. Dereniak, "Uncooled infrared sensor performance", *Proc. SPIE 1993*, Vol.2020, pp.363-378, San Diego, USA.

[35] V.Y. Zerov, V.G. Malyarov, I.A. Khrebtov, "Calculational modeling of the main characteristics of an uncooled linear microbolometer array", *Journal of Optical Technology*, Vol.7, No.3, pp.153-157, 2004.

[36] P.W. Kruse, "Can the 300 K radiating background noise limit be attained by uncooled thermal imagers ?", *Proc. SPIE 2004*, Vol.5406, pp.437-446, Orlando, USA.

[37] E. Mottin, A. Bain, J.L. Martin, J.L. Ouvrier-Buffet, S. Bisotto, J.J. Yon, J.L. Tissot, "Uncooled amorphous silicon technology enhancement for 25 μm pixel pitch achievement", *Proc. SPIE 2003*, Vol.4820, pp.200-207, Seattle, USA.

[38] F. Niklaus, C. Jansson, A. Decharat, J.-E. Källhammer, H. Pettersson, G. Stemme, "Uncooled Infrared Bolometer Arrays Operating in a Low to Medium Vacuum Atmosphere: Performance Model and Tradeoffs", *Proc. SPIE 2007*, Vol.6542, pp.1M.1-1M.12, Orlando, USA.

[39] F. Niklaus, A. Decharat, C. Jansson, G. Stemme, "Performance Model for Uncooled Infrared Bolometer Arrays and Performance Predictions of Bolometers Operating at Atmospheric Pressure", *Infrared Physics and Technology*, http://dx.doi.org/10.1016/j.infrared.2007.08.001, 2007, in press.

[40] R. Richwine, R. Balceraka, C. Rapach, K. Freyvogel, A. Soodb, "A comprehensive model for bolometer element and uncooled array design and imaging sensor performance prediction", *Proc. of SPIE 2006*, Vol.6294, pp.62940F1-62940F11.

[41] B. Backer, M. Kohin, A. Leary, R. Blackwell, R. Rumbaugh, "Advances in uncooled technology at BAE systems", *Proc. SPIE 2003*, Vol.5074, pp.548-556, Orlando, USA.

[42] D. Murphy, M. Ray, J. Wyles, J. Asbrock, C. Hewitt, R. Wyles, E. Gordon, T. Sessler, A. Kennedy, S. Baur, D. Van Lue, "Performance improvements for VOx microbolometer FPAs", *Proc. SPIE 2004*, Vol.5406, pp.531-540, Orlando, USA.

[43] R. J. Blackwell, T. Bach, D. O'Donnell, J. Geneczko, M. Joswick, "17 μm pixel 640 x 480 microbolometer FPA development at BAE Systems", *Proc. SPIE 2007*, Vol.6542, pp.65421U, Orlando, USA.

[44] D. Murphy, M. Ray, J. Wyles, C. Hewitt, R. Wyles, E. Gordon, K. Almada, T. Sessler, S. Baur, D. Van Lue, S. Black, "640 × 512 17 μm microbolometer FPA and sensor development", *Proc. SPIE 2007*, Vol.6542, pp.65421Z, Orlando USA.

[45] J.J. Yon, L. Biancardini, J.L. Tissot, L. Letellier, "Infrared microbolometer sensors and their application in automotive safety", *Proc. AMAA 2003*, pp. 1-15, Berlin, Germany.

[46] S. Tohyama, M. Miyoshi, S. Kurashina, N. Ito, T. Sasaki, A. Ajisawa, N. Oda, "New thermally isolated pixel structure for high-resolution uncooled infrared FPAs", *Proc. SPIE 2004*, Vol. 5406, pp. 428-436, Orlando, USA.

[47] D. Murphy, M. Ray, J. Wyles, J. Asbrock, C. Hewitt, R. Wyles, E. Gordon, T. Sessler, A. Kennedy, S. Baur, D. Van Lue, "Performance improvements for VOx microbolometer FPAs", *Proc. SPIE 2004*, Vol. 5406, pp. 531-540, Orlando, USA.

[48] F. Niklaus, J. Pejnefors, M. Dainese, M. Haggblad, P.-E. Hellström, U.J. Wallgren, G. Stemme, "Characterization of transfer-bonded silicon bolometer arrays", *Proc. SPIE 2004*, Vol.5406, pp.521-530, Orlando, USA.

[49] P. Eriksson, J.Y. Andersson, G. Stemme, "Thermal characterization of surface-micromachined silicon nitride membranes for thermal infrared detectors", *Journal of Microelectromechanical Systems*, Vol.6, No.1, pp.55-61, 1997.

[50] S. Eminoglu, D. Sabuncuoglu Tezcan, M.Y. Tanrikulu, T. Akin, "Low-cost uncooled infrared detectors in CMOS process", *Sensors & Actuators A*, Vol.109, pp.102-113, 2003.

[51] F. Niklaus, E. Kälvesten, G. Stemme, "A new concept for CMOS-compatible fabrication of uncooled infrared focal plane arrays using wafer-scale device transfer bonding", *Proc. SPIE 2001*, Vol.4369, pp.397-404, Orlando, USA.

[52] F. Niklaus, E. Kälvesten, G. Stemme, "Wafer-level membrane transfer bonding of polycrystalline silicon bolometers for use in infrared focal plane arrays", *Journal of Micromechanics and Microengineering*, Vol.11, pp.509-513, 2001.

[53] J.-E. Källhammer, H. Pettersson, D. Eriksson, S. Junique, S. Savage, C. Vieider, J.Y. Andersson, F. Niklaus, G. Stemme, "Fulfilling the pedestrian protection directive using a long-wavelength infrared camera designed to meet the performance and cost targets", *Proc. SPIE 2006*, Vol.6198, pp.74-84, Strasbourg, France.

[54] C. Vieider, S. Wissmar, P. Ericsson, U. Halldin, F. Niklaus, G. Stemme, J.-E. Källhammer, H. Pettersson, D. Eriksson, H. Jakobsen, T. Kvisterøy, J. Franks, J. VanNylen, H. Vercammen, A. VanHulsel, "Low-cost far infrared bolometer camera for automotive use", *Proc. SPIE 2007*, Vol.6542, pp.1L.1-1L.10, Orlando, USA.

[55] T. Kvisterøy, H. Jakobsen, C. Vieider, S. Wissmar, P. Ericsson, U. Halldin, F. Niklaus, F. Forsberg, G. Stemme, J.-E. Källhammer, H. Pettersson, D. Eriksson, J. Franks, J. VanNylen, H. Vercammen, A. VanHulsel, "Far infrared low-cost uncooled bolometer for automotive use", *Proc. AMAA 2007*, Berlin, Germany.

[56] F. Niklaus, G. Stemme, J.-Q. Lu, R.J. Gutmann, "Adhesive wafer bonding", *Journal of Applied Physics: Applied Physics Reviews*, Vol. 99, No. 3, pp.031101/1-031101/28, 2006.

[57] C. Chen, X. Yi, J. Zhang et al., "Micromachined uncooled IR bolometer linear array using VO2 thin films", *International Journal of Infrared and Millimeter Waves* , Vol.22, No.1, pp.53-58, 2001.

[58] C. Chang-hong, Y. Xin-jian, X. Bi-feng, "Infrared responsivity of uncooled VO~2-based thin films bolometer", *Acta physica Sinica.*, Vol.50, Part 3, pp.450-452, 2001.

[59] N. Oda, Y. Tanaka, T. Sasaki, A. Ajisawa, A. Kawahara, S. Kurashina, "Performance of 320 x 240 bolometer-type uncooled infrared detector", *NEC Research & Development.*, Vol.44, No.2, 2003.

[60] S. Chen, H. Ma, S. Xiang, X. Yi, "Fabrication and performance of microbolometer arrays based on nanostructured vanadium oxide thin films", *Smart Mater. Struct.*, Vol.16, pp.696-700, 2007.

[61] R. T. R. Kumar, B. Karunagaran, D. Mangalaraj, S. K. Narayandass, P. Manoravi, M. Joseph and V. Gopal, "Study of a pulsed laser deposited vanadium oxide based microbolometer array", *Smart Mater. Struct.*, Vol.12, pp.188-192, 2003.

[62] Y-H. Han, I.-H, Choi, H-K. Kang, J.-Y. Park, K-T. Kim, H-J. Shin and S. Moon, "Fabrication of vanadium oxide thin film with high-temperature coefficient of resistance using V2O5/V/V2O5 multi-layers for uncooled microbolometers", *Thin Solid Films*, Vol.425, No.1-2, pp.260-264, 2003.

[63] Y. Lv, M. Hu, M. Wu and Z. Liu, "Preparation of vanadium oxide thin films with high temperature coefficient of resistance by facing targets d.c. reactive sputtering and annealing process", *Surface and Coating Technology*, Vol. 201, pp.4969-4972, 2007.

[64] Y-H. Han, K-T. Kim, H-J. Shin, S. Moon, "Enhanced characteristics of an uncooled microbolometer using vanadium-tungsten oxide as a thermometric material", *Applied Physics Letters*, Vol.86, pp.254101-3, 2005.

[65] N. Chi-Anh, H-J. Shin, K. Kim et. al., "Characterization of uncooled bolometer with vanadium tungsten oxide infrared active layer", *Sensors and Actuators A: Physical*, Vol.123, pp.87-92, 2005.

[66] N. Chi-Anh, S. Moon: "Excess noise in vanadium tungsten oxide bolometric material", *Infrared Physics & Technology*, Vol.50, No.1, pp.38-41, 2007.

[67] M. Soltani, M. Chaker, E. Haddad, R. V. Kruzelecky, J. Margot, " Effects of Ti–W codoping on the optical and electrical switching of vanadium dioxide thin films grown by a reactive pulsed laser deposition", *Applied Physics Letters*, Vol.85, No.11, pp.1958-1960, 2004.

[68] A. J. Sylaios, T. R. Schimert, R. W. Gooch, W. L. McCardel, B. A. Ritchey, J. H. Tregilgas, "Amorphous silicon microbolometer technology", *Proc. MRS 2000*, Vol.609, A14.4.1-6.

[69] A. Heredia, F.J. De la Hidalga, A. Torres, A. Jaramillo, "Low temperature electrical properties of a boron-doped amorphous silicon bolometer", *Proc. The Electrochemical Society 2003*, Abs.881.

[70] L. Dong, R. Yue, L. Liu, "Fabrication and characterization of integrated uncooled infrared sensor arrays using a-Si thin-film transistors as active elements", *Journal of Microelectromechanical Systems*, Vol.14, No.5, pp.1167-1177, 2005.

[71] L. Dong, R.F. Yue, L.T. Liu, "A high performance single-chip uncooled a-Si TFT infrared sensor", *Proc. Transducers 2003*, Vol.1, pp.312- 315.

[72] M. Mansi, M. Brookfield, S. Porter, I. Edwards, B. Bold, J. Shannon, P. Lambkin, A. Mathewson. "AUTHENTIC: a very low-cost infrared detector and camera system", *Proc. SPIE 2003*, Vol.4820, pp.227-238.

[73] A. Tanaka, S. Matsumoto, N. Tsukamoto, S. Itoh, K. Chiba, T. Endoh, A. Nakazato, K. Okuyama, Y. Kumazawa, M. Hijikawa, H. Gotoh, T. Tanaka, N. Teranishi, "Infrared focal plane array incorporating silicon IC process compatible bolometer", *IEEE Transactions on Electron Devices*, Vol.43, No.11, pp.1844-1850, 1996.

[74] E. Iborra, M. Clement, L. Herrero, "Sangrador IR uncooled bolometers based on amorphous GeSiO on silicon micromachined structures", *Journal of Microelectromechanical Systems*, Vol.11, No.4, , pp.322-329, 2002.

[75] D. Butler, M. Rana, "Radio Frequency sputtered SiGe and SiGeO thin films for uncooled infrared detectors", *Thin Solid Films*, Vol.514, No.1-2, pp.355-360, 2006.

[76] A. Ahmed, R. Tait, "Noise behavior of amorphous GeSiO for microbolometer applications", *Infrared Physics and Technology*, Vol.46, No.6, pp.468-472, 2005.

[77] M. Moreno, A. Kosarev, A. Torres, R. Ambrosio, "Fabrication and performance comparison of planar and sandwich structures of micro-bolometers with Ge thermo-sensing layer", *Thin Solid Films*, Vol.515, No.19, pp.76070-7610, 2007.

[78] V. Leonov, N. Perova, P. De Moor, B. Du Bois, C. Goessens, B. Grietens, A. Verbist, C. Van Hoof, J. Vermeiren, "Micromachined poly-SiGe bolometer arrays for infrared imaging and spectroscopy", *Proc. SPIE 2003,* Vol.4945, pp.54-63.

[79] I. Chistokhin, I. Michailovsky, B. Fomin, E. Cherepov, "Polycrystalline layers of silicon-germanium alloy for uncooled IR bolometers", *Proc. SPIE 2003,* Vol.5126, No.1, pp.407-414.

[80] R. Yue, L. Dong; L. Liu, "Monolithic uncooled 8 × 8 bolometer arrays based on poly-SiGe thermistor", *International Journal of Infrared and Millimeter Waves*, Vol.27, No.7, pp.995-1003.

[81] S. Wissmar, L. Hoglund, J. Andersson, C. Vieider, S. Susan, P. Ericsson, "High signal to noise ratio quantum well bolometer materials", *Proc. SPIE 2006*, Vol.6401, Stockholm, Sweden.

[82] T. Ichihara, Y. Watabe, Y. Honda, K. Aizawa, "A high performance amorphous Si1-xCx:H thermistor bolometer based on micro-machined structure", Proc. *Tranducers 1997, Vol.2,* pp.1253-1256.

[83] H. Lee, S. Myong, K. Lim, E. Yoon, "Electrical properties of photo-CVD boron-doped hydrogenated nanocrystalline silicon-carbide (p-nc-SiC:H) films for uncooled IR bolometer applications", *Journal of non-crystalline solids*, Vol.316, No.2, pp.297-302, 2003.

[84] M. Almasri, Z. Celik-Butler, D. Butler, A. Yaradanakul, A. Yildiz, "Semiconducting YBaCuO microbolometers for uncooled broad-band IR sensing", *Proc. of the SPIE 2001,* Vol.4369, pp.264-73.

[85] L. Phong, S. Qiu, "Room temperature YBaCuO microbolometers" *Journal of Vacuum Science and Technology, Part A: Vacuum, Surfaces and Films*, Vol.18, No.2, pp.635-638, 2000.

[86] J. Kim, A. Grishin, "Free-standing epitaxial La1-x(Sr,Ca)xMnO3 membrane on Si for uncooled infrared microbolometer", *Applied Physics Letters,* Vol.87, No.3, pp.33502-1-318, 2005.

[87] M. Liger, Y-C. Tal, "A 32*32 parylene-pyrolyzed carbon bolometer imager", *Proc. MEMS 2006, p*p.106-109.

[88] X. He, G. Karunasiri, T. Mei, W. J. Zeng, P. Neuzil, U. Sridhar, "Performance of microbolometer focal plane arrays under varying pressure", *Electron Device Letters*, Vol.21, No.5, pp.233-235, 2000.

[89] V.K. Lindroos, M. Tilli, A. Lehto, T. Motooka: *Handbook of Silicon Based MEMS Materials and Technologies*, to be published by William Andrew Publishing, 2008.

[90] C. Jansson, U. Ringh, K. Liddiard, "Theoretical analysis of pulse bias heating of bolometers and effectiveness of pulse bias compensation", *Proc. SPIE 1995*, Vol.2552, pp.644-653, San Diego, USA.

[91] C. Jansson, U. Ringh, K. Liddiard, N. Robinson, "FOA/DSTO uncooled IRFPA development", *Proc. SPIE 1999*, Vol.3698, pp.264-275, Orlando, USA.

[92] W.J. Parrish, T. Woolaway, "Improvements in uncooled systems using bias equalization", *Proc. SPIE 1999*, Vol.3698, pp.748-755, Orlando, USA.

[93] P. Manning, J. Gillham, N. Parkinson, T. Kaushal, "Silicon foundry micro-bolometers - The route to the mass-market thermal imager", *Proc. of SPIE 2004,* Vol.5406, pp.465-472.

[94] C. Trouilleau, B. Fieque, J. Tissot, P. Robert, A.Crastes, C. Minassian, O.Legras, B. Dupont, A.Touvignon, S. Tinnes, J. Yon, A. Arnaud, "Uncooled amorphous silicon 160 x 120 IRFPA with 25 μm pixel-pitch for large volume applications", *Proc. SPIE 2007*, Vol.6542, pp.1V.1-1V.8, Orlando, USA.